*ICIC Express Letters*
Volume **11**, Number **4**, April **2017**

ICIC International ©2017 ISSN 1881-803X
pp. 763–771

# AN ADAPTIVE SLIDING-MODE SPEED OBSERVER FOR INDUCTION MOTOR UNDER BACKSTEPPING CONTROL

Chiheb Ben Regaya[1], Fethi Farhani[2], Abderrahmen Zaafouri[3] and Abdelkader Chaari[3]

[1]Institute of Applied Sciences and Technology (ISSATGF)
University of Gafsa
Campus Universitaire Sidi Ahmed Zarrouk BP 116-2112 Gafsa, Tunisia
chiheb_ben_regaya@yahoo.fr

[2]National Engineering School of Gafsa
University of Gafsa
Sidi Ahmed Zarroug BP 2100 Gafsa, Tunisia
f.farhani@live.fr

[3]Higher National Engineering School of Tunis (ENSIT)
University of Tunisia
5 Av. Taha Hussein, BP 56, 1008 Tunis, Tunisia
abderrahmen.zaafouri@isetr.rnu.tn; assil.chaari@esstt.rnu.tn

Received September 2016; accepted December 2016

Abstract. *In this paper, the induction machine is controlled by a Multiple-Input Multiple-Output (MIMO) Backstepping controller. To eliminate speed sensor we use a sliding mode observer. The control algorithm and observation are emphasized by simulation tests. Analysis of the obtained results shows the characteristic robustness to disturbances of the load and to the speed reference changing.*
**Keywords:** Induction motor, Backstepping control, Sliding mode observer, Speed sensorless, Vector control

1. **Introduction.** Vector control technique applied to induction motors allowed to have performances comparable to those of the DC motor, in which the torque and flux are decoupled and independently controlled, to obtain a good control accuracy and high dynamic performance. However, vector control has the disadvantage of requiring the use of a speed sensor, which imposes additional costs and increases the complexity of the arrangements [1-3]. To overcome this drawback, many controls techniques have been proposed in the literature. In the past decade, a wide range of nonlinear methods for feedback control, state estimation, and parameter identification has merged. Among them, Backstepping control gained wide acceptance because this control technique can offer many good properties, such as insensitivity to parameter variations, external disturbance rejection, and fast dynamic response [4-8]. The Backstepping is one of nonlinear control techniques recently appeared. Its principle is to decompose the overall system prime subsystems. These subsystems are cascaded to establish successive causal relationships. With this structure, we can ensure the construction of an iterative and systematic control of the system of law from virtual control laws well defined. Indeed, every step of the synthesis process, a virtual command is generated for the convergence of each subsystem to their equilibrium state [9,10]. Various technical controls without speed sensor were presented in the literature, such as adaptive speed observer [11], MRAS speed estimator [12], fuzzy logic speed observer [13], backstepping observer [1] and sliding mode speed observer [14]. These solutions cited above show that the estimation error of the rotor speed converges approximately to 10% of the nominal value and does not guarantee a high performance

of speed control. To overcome this drawback, this paper presents after the Backstepping control, a speed observation system, which comprises a current observer, a rotor flux observer and a rotor speed observer, that is presented for the speed sensorless control of the induction motor. The present article is organized as follows. In Section 2, the model of induction motor is defined. The Backstepping control is established in Section 3. In Section 4, the sliding mode observer of rotor flux and speed estimation is developed. Section 5 is dedicated to the simulations results using MATLAB-SIMULINK environment with some comments to conclude this work. We close our article with a conclusion.

2. **Induction Motor Modelling.** The equations of the machine in a reference related to the rotating field can be written in the following form taking account of the orientation of the rotor flux, which means $\phi_{rd} = \phi_r^*$ and $\phi_{rq} = 0$ [15,16].

$$\begin{cases} \dfrac{d}{dt} i_{sd} = f_d + \dfrac{1}{\sigma L_s} v_{sd} \\ \dfrac{d}{dt} i_{sq} = f_q + \dfrac{1}{\sigma L_s} v_{sq} \\ \dfrac{d}{dt} \phi_{rd} = M\beta_r i_{sd} - \beta_r \phi_{rd} \\ \dfrac{d}{dt} \omega_r = k_c \phi_{rd} i_{sq} - \dfrac{f}{J}\omega_r - \dfrac{C_r}{J} \end{cases} \tag{1}$$

where $f_d = -\gamma_1 i_{sd} + n_p \omega_r i_{sq} + k\beta_r \phi_{rd} + L_m \beta_r \frac{i_{sq}^2}{\phi_{rd}}$, $f_q = -\gamma_1 i_{sq} - n_p \omega_r i_{sd} - kn_p \omega_r \phi_{rd} - L_m \beta_r \frac{i_{sd} i_{sq}}{\phi_{rd}}$. With $\gamma_1 = \frac{1}{\sigma L_s}\left(R_s + \frac{L_m^2}{L_r^2} R_r\right)$, $\beta_r = \frac{1}{\tau_r}$, $k = \frac{L_m}{\sigma L_s L_r}$, $k_c = \frac{3}{2}\frac{n_p L_m}{J L_r}$.

3. **Backstepping Control Strategy.** The aim of the command to be designed is to force the rotor speed and flux to follow their references. To achieve this, we will look for a Lyapunov function that allows the stabilization of the subsystem described by the third and fourth terms of Equation (1) [17,18]. In this case, the tracking errors of speed ($e_\omega$), rotor flux ($e_\phi$), direct and quadrature currents $\left(e_{i_{sd}}, e_{i_{sq}}\right)$ are defined as follows:

$$\begin{cases} e_\omega = \omega_r^* - \omega_r \\ e_\phi = \phi_{rd}^* - \phi_{rd} \end{cases} \tag{2}$$

$$\begin{cases} e_{i_{sq}} = i_{sq}^* - i_{sq} \\ e_{i_{sd}} = i_{sd}^* - i_{sd} \end{cases} \tag{3}$$

$i_{sq}^*$ and $i_{sd}^*$ are the virtual stabilizing functions that are going to be designed using the Lyapunov stability theory to achieve the objective of pursuit. By using Equations (2) and (3), the dynamics of speed, flux and stator currents regulation errors can be written as the follows:

$$\begin{cases} \dot{e}_\omega = \dot{\omega}_r^* - k_c \phi_{rd} i_{sq} + \dfrac{C_r}{J} + \dfrac{f}{J}\omega_r \\ \dot{e}_\phi = \dot{\phi}_{rd}^* - M\beta_r i_{sd} + \beta_r \phi_{rd} \end{cases} \tag{4}$$

$$\begin{cases} \dot{e}_{i_{sq}} = \dot{i}_{sq}^* - f_q - \dfrac{1}{\sigma L_s} v_{sq} \\ \dot{e}_{i_{sd}} = \dot{i}_{sd}^* - f_d - \dfrac{1}{\sigma L_s} v_{sd} \end{cases} \tag{5}$$

With an appropriate choice of the Lyapunov functions of the subsystems described by Equations (4) and (5), the virtual stabilizing functions and the stator voltage control law are given by the following equations:

$$\begin{cases} i_{sq}^* = \dfrac{1}{k_c\phi_{rd}}\left(k_\omega e_\omega + \dot{\omega}_r^* + \dfrac{C_r}{J} + \dfrac{f}{J}\omega_r\right) \\ i_{sd}^* = \dfrac{1}{M\beta_r}\left(k_\phi e_\phi + \dot{\phi}_{rd}^* + \beta_r\phi_{rd}\right) \end{cases} \tag{6}$$

$$\begin{cases} v_{sq}^* = \sigma L_s\left(k_{i_{sq}}e_{i_{sq}} + \dot{i}_{sq}^* - f_q\right) \\ v_{sd}^* = \sigma L_s\left(k_{i_{sd}}e_{i_{sd}} + \dot{i}_{sd}^* - f_d\right) \end{cases} \tag{7}$$

The proof is given in Appendix A.

4. **Sliding Mode Observer of the Rotor Speed.** The structure of the sliding mode observer does not require knowledge speed and rotor resistance, unlike other observers [19-22]. This advantage allows the sliding mode observer to provide a good estimate of the rotor flux and the stator currents even under variation of these quantities. In addition, the use of sliding mode methods for the design of the observer ensures respectively robustness with respect to various disturbances, and good dynamic performance over the entire speed range. The equations of the induction motor in a reference connected to the stator ($\alpha\_\beta$) are given by the following equation:

$$\begin{cases} \dfrac{d}{dt}i_s = \eta A'\phi_r + \gamma i_s + B_1 v_s \\ \dfrac{d}{dt}\phi_r = -\left(A'\phi_r - A'' i_s\right) \end{cases} \tag{8}$$

where $i_s = \begin{bmatrix} i_{s\alpha} & i_{s\beta} \end{bmatrix}^T$, $\phi_r = \begin{bmatrix} \phi_{r\alpha} & \phi_{r\beta} \end{bmatrix}^T$, $v_s = \begin{bmatrix} v_{s\alpha} & v_{s\beta} \end{bmatrix}^T$, $B_1 = \begin{bmatrix} \frac{1}{\sigma L_s} & 0 \\ 0 & \frac{1}{\sigma L_s} \end{bmatrix}$, $A = \begin{bmatrix} \beta_r & \omega_r \\ -\omega_r & \beta_r \end{bmatrix}$, $A'' = \frac{R_r L_m}{L_r}$.

We can see that the $A'\phi_r$ term appears in the equations of the current and flux of the induction motor. So, in this model the coupling terms between the $\alpha$ and $\beta$ axes are exactly the same, and can be replaced by the same sliding function $U$ in the system of Equation (8). The function $U$ is defined by the following matrix:

$$U = A'\phi_r = \begin{bmatrix} \beta_r & \omega_r \\ -\omega_r & \beta_r \end{bmatrix}\begin{bmatrix} \phi_{r\alpha} \\ \phi_{r\beta} \end{bmatrix} \tag{9}$$

Using Equation (9), the equations of the stator currents and rotor flux observers can be defined by the following matrix representation:

$$\begin{cases} \dfrac{d}{dt}\hat{i}_s = \eta U + \gamma\hat{i}_s + B_1 v_s \\ \dfrac{d}{dt}\hat{\phi}_r = -U + A''\hat{i}_s \end{cases} \tag{10}$$

where $\hat{i}_s = \begin{bmatrix} \hat{i}_{s\alpha} & \hat{i}_{s\beta} \end{bmatrix}^T$, $\hat{\phi}_r = \begin{bmatrix} \hat{\phi}_{r\alpha} & \hat{\phi}_{r\beta} \end{bmatrix}^T$, $U = \begin{bmatrix} U_{r\alpha} & U_{r\beta} \end{bmatrix}^T$, $U_{r\alpha} = -k' sign\left(S_{s\alpha}\right)$, $U_{r\beta} = -k' sign\left(S_{s\beta}\right)$.

With $S_{s\alpha} = \widetilde{i}_{s\alpha} = \hat{i}_{s\alpha} - i_{s\alpha}$, $S_{s\beta} = \widetilde{i}_{s\beta} = \hat{i}_{s\beta} - i_{s\beta}$.

The sliding functions $U_{r\alpha}$ and $U_{r\beta}$ depend only on the error between the estimated and measured currents of each axis. When the estimation error converges to zero, the components of the rotor flux along the axes $\alpha$ and $\beta$ are a simple integration of the $\left(-U + A'' i_s\right)$ term. Thus, observers designed for currents and flux have no coupling between them, which makes the observation models of currents and flux completely decoupled.

When the system reaches the sliding surface, this means that the observed currents converge to those measured. In this case, the flux estimation is just an integration of the sliding functions and the stator currents without needing other information related to motor parameters or the rotor speed. The equivalent control of the observer is difficult to implement, which is why it is reasonable to assume that the latter is achieved by using a low-pass filter of the discontinuous control [23].

$$\begin{bmatrix} U_{r\alpha}^{eq} \\ U_{r\alpha}^{eq} \end{bmatrix} = \begin{bmatrix} \dfrac{1}{\tau s+1} & 0 \\ 0 & \dfrac{1}{\tau s+1} \end{bmatrix} \begin{bmatrix} U_{r\alpha} \\ U_{r\beta} \end{bmatrix} \tag{11}$$

where $\tau$ is the time constant of the low pass filter.

In case where the observed currents converge to those measured, the rotor flux can be calculated from the second term of Equation (10). The rotor speed can be estimated using the stator currents and rotor flux from the sliding mode observer. According to the systems of Equations (9), (10) and (11) we can write:

$$\begin{bmatrix} U_{r\alpha}^{eq} \\ U_{r\beta}^{eq} \end{bmatrix} = \begin{bmatrix} \beta_r & \hat{\omega}_r \\ -\hat{\omega}_r & \beta_r \end{bmatrix} \begin{bmatrix} \hat{\phi}_{r\alpha} \\ \hat{\phi}_{r\beta} \end{bmatrix} \tag{12}$$

According to the system of Equation (12), we can get the following expression:

$$\begin{bmatrix} \beta_r \\ \hat{\omega}_r \end{bmatrix} = \frac{1}{\left|\hat{\phi}_{r\alpha}^2 + \hat{\phi}_{r\beta}^2\right|} \begin{bmatrix} \hat{\phi}_{r\alpha} & \hat{\phi}_{r\beta} \\ \phi_{r\beta} & -\hat{\phi}_{r\alpha} \end{bmatrix} \begin{bmatrix} U_{r\alpha}^{eq} \\ U_{r\beta}^{eq} \end{bmatrix} \tag{13}$$

Using Equation (13), we can finally calculate the estimated value of the rotor speed as follows:

$$\hat{\omega}_r = \frac{1}{\left|\hat{\phi}_{r\alpha}^2 + \hat{\phi}_{r\beta}^2\right|} \left(\hat{\phi}_{r\beta} U_{r\alpha}^{eq} - \hat{\phi}_{r\alpha} U_{r\beta}^{eq}\right) \tag{14}$$

The block diagram of the sliding mode observer is given by the figure below.

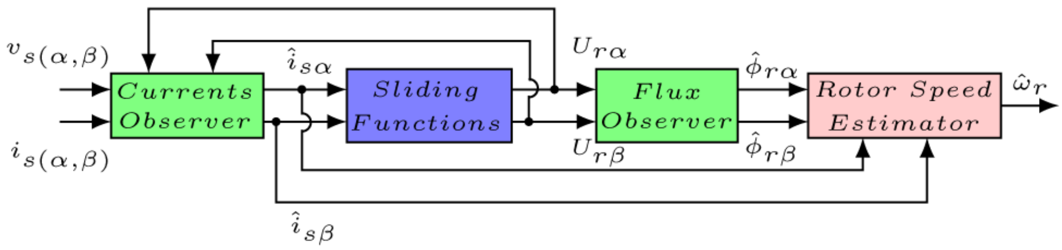


FIGURE 1. Block diagram of the sliding mode observer

5. **Simulation Results and Discussion.** In order to validate the proposed control algorithm, we simulate the Backstepping control presented in Section 3 with an adaptive sliding mode speed observer, where it will replace the sensor signals from the flux and speed with those generated by the designed observers. The simulation results have been obtained by implementing the control scheme illustrated by Figure 2 under the Matlab-Simulink environment with 50$\mu$s sampling period. The motor parameters values are given in Table 1. The two reference speed profiles illustrated by Figures 3(a) and 3(b) are considered to verify the effectiveness of the proposed control algorithm. For the first and second tests a load torque disturbance equal to 10Nm is applied between $t = 2$s and $t = 4$s. For all tests, the rotor flux reference is equal to 0.75Wb.

The simulation results for the two used reference speed profiles are shown in Figures 4(a)-5(d). In Figures 4(a) and 5(a), it can be seen that the Backstepping technique guarantees a good speed tracking. One notices a small decrease in rotor speed (almost negligible) when the torque load is applied.

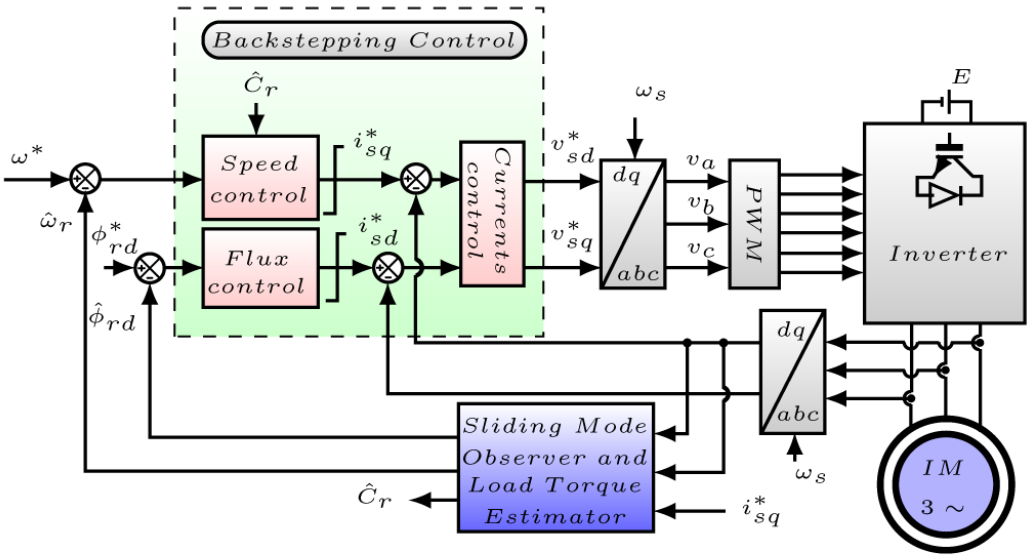


FIGURE 2. Bloc scheme of the Backstepping control of IM with sliding mode speed observer

TABLE 1. Motor parameters values

| Symbol | | Quantity | UM |
|---|---|---|---|
| $R_s$ | Stator resistance | 2.3 | [Ω] |
| $R_r$ | Rotor resistance | 1.83 | [Ω] |
| $L_s$ | Stator inductance | 261 | [mH] |
| $L_r$ | Rotor inductance | 261 | [mH] |
| $M$ | Mutual inductance | 245 | [mH] |
| $\sigma$ | Leakage factor | 0.134 | – |
| $J$ | Moment of inertia | 0.22 | [Kgm$^2$] |
| $f$ | Friction coefficient | 0.001 | – |
| $V_n$ | Rated voltage | 380 | [V] |
| $I_n$ | Rated current | 10.4 | [A] |
| $P_n$ | Rated power | 3 | [kW] |
| $n_p$ | Number of pole pairs | 2 | – |

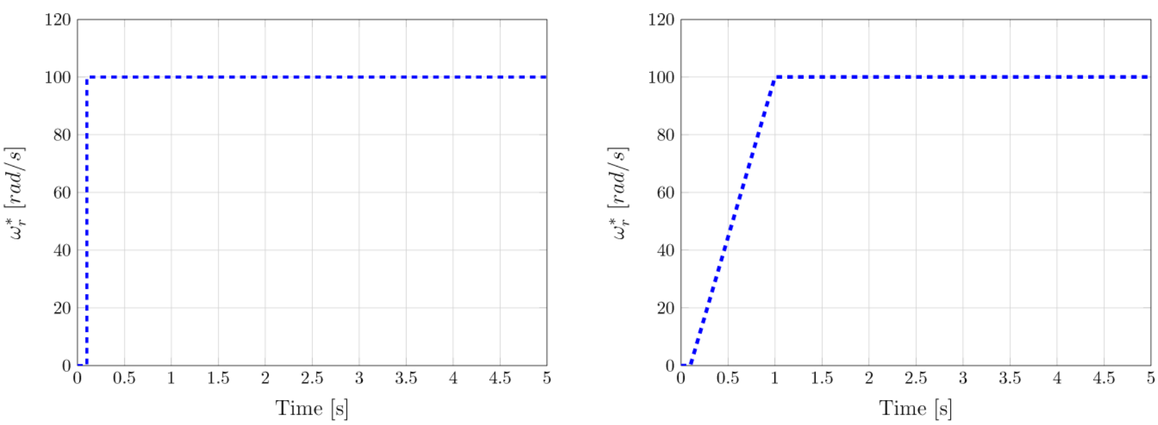


(a) Reference speed: Profile 1 (High dynamic) (b) Reference speed: Profile 2 (Slow dynamic)

FIGURE 3. Reference speed profiles

Figures 4(b) and 5(b) show the error between real and estimated speed. The rotor speed estimation error does not exceed 2% of the reference speed for the two used speed reference profiles. The real and estimated rotor flux along the $\alpha$ axis are illustrated by Figures 4(c) and 5(c). Figures 4(d) and 5(d) demonstrate that the adaptive Backstepping control can guarantee a good estimation of the rotor flux, with an accuracy of up to 98%.

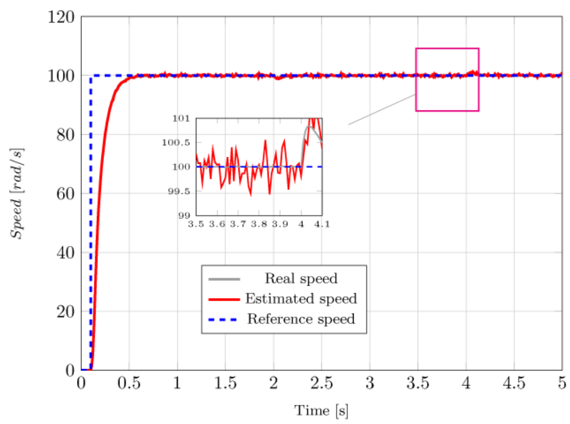


(a) Real, measured and estimated speed (Profile 1)

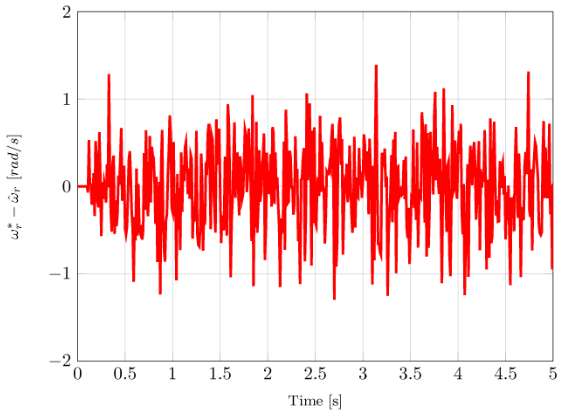


(b) Rotor speed estimation error (Profile 1)

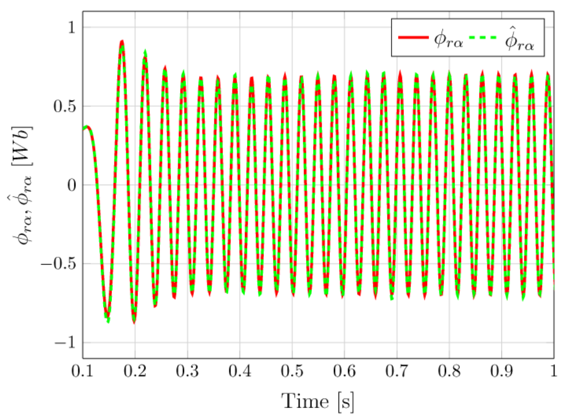


(c) Real and estimated flux along the $\alpha$ axis (Profile 1)

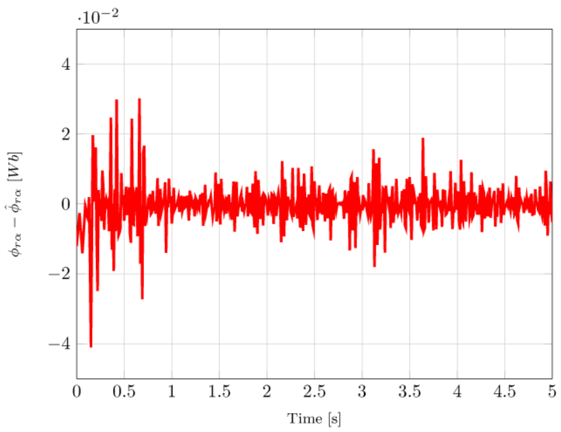


(d) Rotor flux estimation error along the $\alpha$ axis (Profile 1)

FIGURE 4. Simulation results with the first speed profile (Profile 1)

The different simulation results have shown that the adaptive Backstepping control using a sliding mode speed observer has realized a good dynamic and performance for motor monitoring. The efficacity of the rotor flux and speed sensorless control is proved by extensive simulation results.

6. **Conclusions.** A Backstepping control and speed estimation algorithm based on sliding mode currents and flux observers is developed in this paper. In the observation algorithm, sliding mode functions are selected to estimate rotor speed that is assumed to be unknown. The proposed scheme was validated by many simulation tests to confirm the theoretical concepts. This method has successfully demonstrated the speed sensorless control of induction motor using only the stator currents and voltages measurements. The future work will focus on the real implementation of the proposed scheme using a dSpace DS1104 with main processor (MPC8240, Power PC603e core, 250MHz) and slave DSP subsystem from Texas Instruments (DSP TMS320F240).

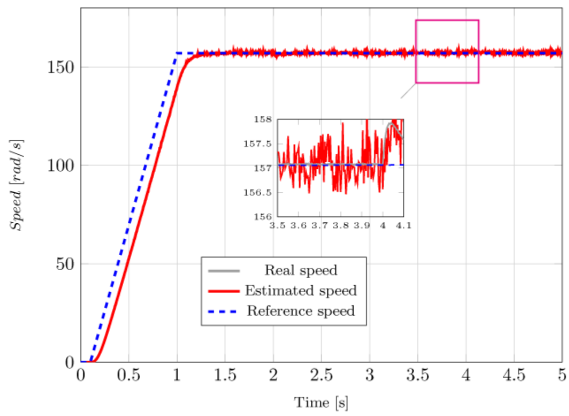


(a) Real, measured and estimated speed (Profile 2)

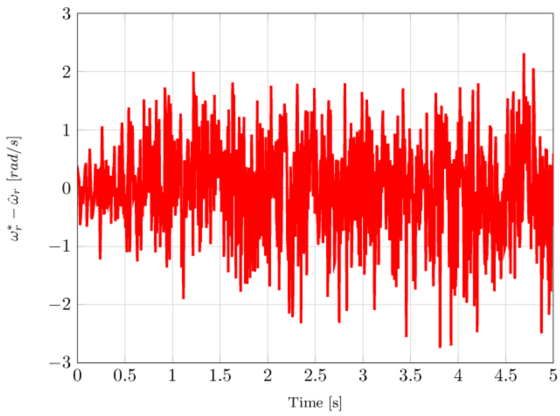


(b) Rotor speed estimation error (Profile 2)

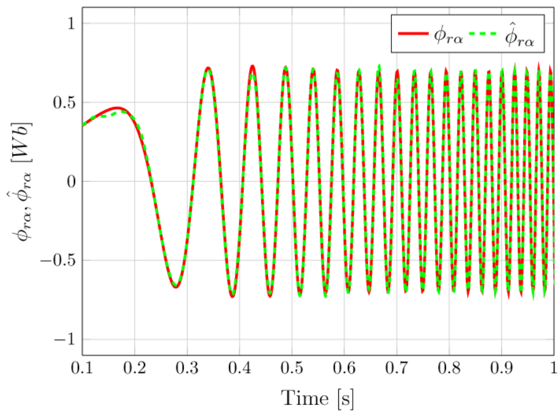


(c) Real and estimated flux along the $\alpha$ axis (Profile 2)

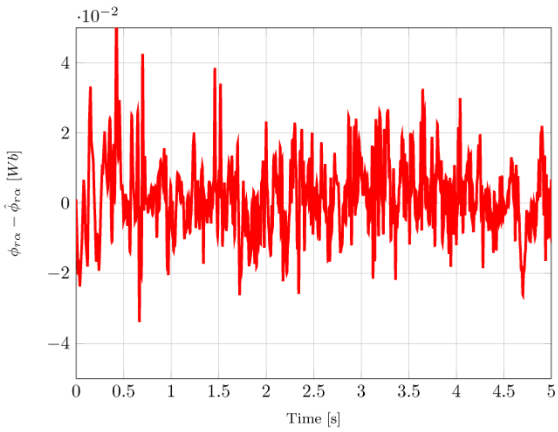


(d) Rotor flux estimation error along the $\alpha$ axis (Profile 2)

FIGURE 5. Simulation results with the second speed profile (Profile 2)

## REFERENCES


[1] D. Traore, J. d. Leon and A. Glumineau, Adaptive interconnected observer-based backstepping control design for sensorless induction motor, *Automatica*, vol.48, no.4, pp.682-687, 2012.

[2] S. Gong and Z. Li, Induction motor vector control based on adaptive identification of rotor resistance, *Proc. of the International Conference on Control Engineering and Communication Technology*, pp.145-148, 2012.

[3] A. El Fadili, F. Giri, A. El Magri, R. Lajouad and F. Z. Chaoui, Adaptive control strategy with flux reference optimization for sensorless induction motors, *Control Engineering Practice*, vol.2014, no.26, pp.91-106, 2014.

[4] D. Traore, J. d. Leon and A. Glumineau, Sensorless induction motor adaptive observer-backstepping controller: Experimental robustness tests on low frequencies benchmark, *IET Control Theory & Applications*, vol.4, no.10, pp.1989-2002, 2010.

[5] F. Mehazzem, A. L. Nemmour, A. Reama and H. Benalla, Nonlinear integral backstepping control for induction motors, *International Aegean Conference on Electrical Machines and Power Electronics and Electromotion Joint Conference*, pp.826-850, 2011.

[6] A. Zaafouri, C. Ben Regaya and A. Chaari, Backstepping approach applied for control and on-line adaptation of the rotor resistance, *World Applied Sciences Journal*, vol.28, no.8, pp.1120-1126, 2013.

[7] S. M. J. R. Fatemi, N. R. Abjadi, J. Soltani and S. Abazari, Speed sensorless control of a six-phase induction motor drive using backstepping control, *IET Power Electronics*, vol.7, no.1, pp.114-123, 2013.

[8] A. Zaafouri, C. B. Regaya, H. B. Azza and A. Chari, DSP-based adaptive backstepping using the tracking errors for high-performance sensorless speed control of induction motor drive, *ISA Transactions*, vol.60, pp.333-347, 2016.

[9] C. Ben Regaya, F. Farhani, A. Zaafouri and A. Chaari, Backstepping control of an induction motor, *International Conference on Computer Related Knowledge*, pp.1-3, 2012.
[10] C. Ben Regaya, A. Zaafouri and A. Chaari, Loss-minimizing with backstepping technique control for induction motors and on line adaptation of the stator and rotor resistance, *Middle-East Journal of Scientific Research*, vol.15, no.3, pp.389-397, 2013.
[11] H. Kubota, I. Sato, Y. Tamura, K. Matsuse, H. Ohta and Y. Hori, Regenerating-mode low-speed operation of sensorless induction motor drive with adaptive observer, *IEEE Trans. Industry Applications*, vol.38, no.4, pp.1081-1086, 2002.
[12] H. M. Kojabadi, L. Chang and R. Doraiswami, A MRAS-based adaptive pseudoreduced-order flux observer for sensorless induction motor drives, *IEEE Trans. Power Electronics*, vol.20, no.4, pp.930-938, 2005.
[13] A. A. Adam and K. Gulez, Fast response adaptive fuzzy logic controller for sensorless direct torque control of PMSM with minimum torque ripple, *COMPEL: The International Journal for Computation and Mathematics in Electrical and Electronic Engineering*, vol.27, no.2, pp.534-550, 2008.
[14] R. P. Vieira, C. C. Gastaldini, R. Z. Azzolin and H. A. Grundling, Discrete-time sliding mode speed observer for induction machine drives, *Proc. of the 11th Brazilian Power Electronics Conference*, pp.213-218, 2011.
[15] D. Casadei, F. Profumo, G. Serra and A. Tani, FOC and DTC: Two viable schemes for induction motors torque control, *IEEE Trans. Power Electronics*, vol.17, no.5, pp.779-787, 2002.
[16] F. Farhani, C. Ben Regaya, A. Zaafouri and A. Chaari, A quasi linear parameter varying approach to robust control of an induction machine, *International Multi-Conference on Systems, Signals & Devices*, pp.1-5, 2013.
[17] F.-J. Lin, P.-H. Shen and S.-P. Hsu, Adaptive backstepping sliding mode control for linear induction motor drive, *IEE Proceedings – Electric Power Applications*, vol.149, no.3, pp.184-194, 2002.
[18] M. Horch, A. Boumdine and L. Baghli, Backstepping approach for nonlinear super twisting sliding mode control of an induction motor, *International Conference on Control, Engineering Information Technology*, pp.1-6, 2015.
[19] Z. Wei and J. J. Luo, Speed and rotor flux estimation of induction motors based on extended kalman filter, *The 6th International Conference on Networked Computing and Advanced Information Management*, pp.157-160, 2010.
[20] S. Gadoue, D. Giaouris and J. Finch, MRAS sensorless vector control of an induction motor using new sliding-mode and fuzzy-logic adaptation mechanisms, *IEEE Trans. Energy Conversion*, vol.25, no.2, pp.394-402, 2010.
[21] C.-J. Chiang, Y.-K. Wang and W.-T. Cheng, EKF based rotor and stator resistance estimation in speed sensorless control of induction motors, *American Control Conference*, pp.1174-1179, 2012.
[22] C. Ben Regaya, A. Zaafouri and A. Chaari, Electric drive control with rotor resistance and rotor speed observers based on fuzzy logic, *Mathematical Problems in Engineering*, vol.2014, pp.1-9, 2014.
[23] C. B. Regaya, A. Zaafouri and A. Chaari, A new sliding mode speed observer of electric motor drive based on fuzzy-logic, *Acta Polytechnica Hungarica*, vol.11, no.3, pp.219-232, 2014.

## **Appendix** A.

**Proof:** The Lyapunov function candidate associated to the subsytem defined by Equation (2) can be defined as follows:

$$V_1 = \frac{1}{2}\left(e_\omega^2 + e_\phi^2\right) \tag{15}$$

The derivation of Equation (15) can be expressed as follows:

$$\begin{aligned}\dot{V}_1 &= -k_\omega e_\omega^2 - k_\phi e_\phi^2 + e_\omega \left(k_\omega e_\omega + \dot{\omega}_r{}^* - k_c \phi_{rd} i_{sq} + \frac{C_r}{J} + \frac{f}{J}\omega_r\right) \\ &\quad + e_\phi \left(k_\phi e_\phi + \dot{\phi}_{rd}^* - M\beta_r i_{sd} + \beta_r \phi_{rd}\right)\end{aligned} \tag{16}$$

We consider $i_{sq}^*$ and $i_{sd}^*$ as virtual commands used to control our first subsystem and as a reference for the next subsystem. With a suitable choice of these controls, we will ensure the negativity of the Lyapunov function $\dot{V}_1$. Hence we get the expression of the virtual stabilizing functions given by Equation (6) and guarantee that $\dot{V}_1 = -k_\omega e_\omega^2 - k_\phi e_\phi^2 \leq 0$.

The derivation of Equations (15) can be expressed as follows:

$$\begin{aligned}\dot{V}_1 = & -k_\omega e_\omega^2 - k_\phi e_\phi^2 + e_\omega \left( k_\omega e_\omega + \dot{\omega_r}^* - k_c \phi_{rd} i_{sq} + \frac{C_r}{J} + \frac{f}{J}\omega_r \right) \\ & + e_\phi \left( k_\phi e_\phi + \dot{\phi}_{rd}^* - M\beta_r i_{sd} + \beta_r \phi_{rd} \right)\end{aligned} \tag{17}$$

We consider $i_{sq}^*$ and $i_{sd}^*$ as virtual commands used to control our first subsystem and as a reference for the next subsystem. With a suitable choice of these controls, we will ensure the negativity of the Lyapunov function $\dot{V}_1$. Hence we get the expression of the virtual stabilizing functions given by Equation (6) and guarantee that $\dot{V}_1 = -k_\omega e_\omega^2 - k_\phi e_\phi^2 \leq 0$. The Lyapunov function associated to the overall system is expressed as:

$$V_2 = V_1 + \frac{1}{2}\left( e_{i_{sd}}^2 + e_{i_{sq}}^2 \right) \tag{18}$$

To ensure that the derivative of the Lyapunov function $V_2$ is always negative, we choose the control laws in the form presented by the equation system

$$\begin{cases} v_{sq}^* = \sigma L_s \left( k_{i_{sq}} e_{i_{sq}} + \dot{i}_{sq}^* - f_q \right) \\ v_{sd}^* = \sigma L_s \left( k_{i_{sd}} e_{i_{sd}} + \dot{i}_{sd}^* - f_d \right) \end{cases} \tag{19}$$

with $\dot{V}_2 = \dot{V}_1 - k_{i_{sq}} e_{i_{sq}}^2 - k_{i_{sd}} e_{i_{sd}}^2$.